Research article

Carbon and zeolite-based composites for radionuclide and heavy metal sorption

Darina Smržová [a], Lórant Szatmáry [b], Petra Ecorchard [a,*], Aneta Machálková [a], Monika Maříková [a], Petra Salačová [b], Martin Straka [b]

[a] Institute of Inorganic Chemistry of the Czech Academy of Sciences, Husinec-Řež 1001, 250 68, Řež, Czech Republic
[b] Fuel Cycle Chemistry Department, ÚJV Řež a.s, 250 68, Husinec Řež, Czech Republic

HIGHLIGHTS

- Synthetic zeolite (type A, P or Y) modified by graphene oxide and exfoliated graphite.
- Monitoring of effect of different type of zeolites on sorption.
- Effect of different ratios of individual components.
- Sorption analyses of radionuclides Cs^+ and Sr^{2+} or heavy metals Pb^{2+} and Cd^{2+}.
- Two samples are most suitable as multifunctional sorbents.

GRAPHICAL ABSTRACT
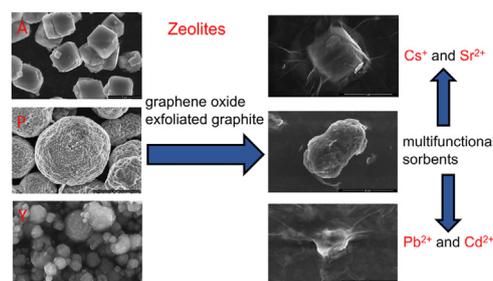
ARTICLE INFO

ABSTRACT

Zeolites have been investigated as sorbents of heavy metals from water. Since graphene oxide was already reported as promising radionuclide sorbent, we developed composite materials containing both a synthetic zeolite (type A, P or Y) and graphene oxide to be multifunctional sorbents. The extension of multifunctionality of sorbents was done by presence of third component, exfoliated graphite, to have additional properties as conductivity. The changing sorption activities of a composite was studied depending on its composition and functional modification. The composites, characterized by X-ray powder diffraction, Raman, FTIR spectroscopy and scanning electron microscopy, were tested for sorption of selected radionuclides ($^{134}Cs^+$, $^{85}Sr^{2+}$) and heavy metals (Pb^{2+}, Cd^{2+}). The dependency on composition was found in connection with a high sorption of Pb^{2+} and Cd^{2+}. Finally, optimized multifunctional sorbents (Gr-GO-COOH-A in ratio 40:40:20 and Gr:GO:A in ratio 25:25:50) were found to keep interesting high sorption activities for heavy metals and radionuclides with good conductivity properties.

1. Introduction

Water pollution by heavy metals and radionuclides is an important environmental issue. The main sources of water pollution by heavy metals are industry and mining [1, 2]. Lead, mercury, copper, cadmium, nickel and chromium are the most common toxic heavy metals found in industrial waters [3, 4]. Heavy metals can accumulate in living organisms and cause various health problems [1, 3]. One of the most harmful heavy metals is inorganic lead in the Pb^{2+} oxidation state; acute poisoning by lead causes dysfunctions in the kidneys, reproductive system, liver, brain and central nervous system [5]. Cadmium is considered to be as toxic as lead [6].

Radionuclides, particularly ^{137}Cs and ^{90}Sr, are also a threat to environment. These isotopes were released to the environment for example from nuclear weapons or nuclear accidents. Moreover, ^{90}Sr is also present in spent nuclear fuel and in radioactive waste from nuclear reactors [7]. When these radionuclides enter human bodies, ^{137}Cs can cause damage or death of cells and cancer while ^{90}Sr can be source of bone cancer and possibly leukemia [7]. Therefore, removal of both isotopes from the environment is desirable.

Sorption seems to be a suitable way for removal of heavy metals and radionuclides. For heavy metals, various types of sorbents have been investigated including activated carbon, natural zeolites, nano zeolites, clay minerals (i.e. bentonite, kaolin), biomaterials (i.e. peat, sawdust) and cheap adsorbents (i.e. agricultural waste, industrial by-products). Zeolites and clays, titanates, vanadates, manganese oxides and other materials were already investigated for sorption of radionuclides [7, 8, 9, 10, 11].

Zeolites are alkaline aluminosilicates with structure composed from primary building units of silicon-aluminum oxygen (tetrahydra) formed to three-dimensional framework containing exchangeable cations (Na$^+$, K$^+$, Ca^{2+} and Mg^{2+}) with water molecules coordinated in the structure. The network includes a complex of rings forming channels and voids with homogeneous and microporous structure [1, 12]. The channels can be used for ion exchange. Moreover, heavy metals can also be removed by adsorption on the surface of micropores [1].

High value of ion exchange capacity, selectivity, low cost and compatibility with natural environment are advantage of natural zeolites [5]; disadvantage is that they are not only composed of pure zeolitic phases and their composition varies depending on location.

The preparation of synthetic zeolites is more expensive but provides materials with high reproducibility and adjustment of physico-chemical properties [13]. Moreover, using natural nanoporous materials such as bentonite and kaolin for zeolite synthesis leads to more affordable adsorbents [14].

Ezzedine et al. reported that synthetic zeolite NaX Faujasite showed high sorption capacity for Pb^{2+}, Cd^{2+} and Cu^{2+}, because of a low Si/Al ratio (~1.18) and a large number of exchangeable Na [4]. A suitable sorbent for Pb sorption is also low silica nano-zeolite X [14]. Heavy metals are removed by synthetic zeolites more likely in acidic up to neutral pH range - for lead is optimal pH 6; for sorption of cadmium was tested pH 3 and 7 and better results were obtained at pH 7 [13].

Many research papers were also published for investigation of radionuclide sorption by zeolites. Several studies focused on comparison of Cs and Sr sorption. Yang et al. prepared sulfur-modified chabazite and observed that Cs$^+$ selectivity increased with sulfur loading [15]. Faghihian et al. prepared magnetic zeolite nanocomposite for removal of both Cs$^+$ and Sr^{2+} from aqueous solution [16].

Lately, carbon-based 2D materials as graphene and graphene oxide were investigated for various applications, including sorbents. Zeolites modified by GO as sorbents for heavy metals have been already reported. Liu et al. modified zeolite NaA through doped thiourea reduced GO and observed enhanced removal of Cd^{2+} [17]. Shi et al. reported hierarchical 13X zeolite/reduced graphene oxide porous material for removal of Pb^{2+} in trace concentrations from drinking water [18]. Although GO/polystyrene composites were previously studied as sorbents of radionuclides by our group [19], no report so far was found for radionuclide sorption on zeolite/GO.

Paste electrodes based on carbon powder and a binder are popular because of their characteristics like high sensitivity, wide potential window, low level of background current, possibilities of modification and also low cost. Different types of carbon are being used for the construction of paste electrodes with graphite being the most common carbon material used, along with carbon nanotubes [20]. However, powder graphene is getting an increased attention nowadays as the basic matrix of the paste electrode design, typically in the form enriched with some specific sorbent. Such a system allows use of the electrode for differential pulse voltametric determination of wide spectrum of analytes depending on the added sorbent [21], and offering some superior characteristics compared to ordinary graphite-based systems [22].

Here, we report composites of synthetic zeolites A, P and Y with graphene/graphene oxide and report sorption efficiency for selected heavy metals (Pb^{2+} and Cd^{2+}) and radionuclides (Cs$^+$ and Sr^{2+}). The studies were focused on different type of zeolites and optimization of the ratio between the active components. Several concentrations of cations (low and high) were selected to test sorption of radionuclides and heavy metals. Based on reports for contaminated water at nuclear accidents [23], concentration of Cs$^+$ and Sr^{2+} can be expected at the lower concentration range. Concentrations of heavy metals in water can vary depending on area, type of water, and source of contamination, for example Ahmad et al. [24] reported 0.30 mg/L Pb^{2+} and 0.02–0.08 mg/L Cd^{2+} for effluent contaminated water in Bangladesh while Guain et al. [25] investigated treatment of mine water containing 0.01 mg/L Pb^{2+} and 0.003 mg/L Cd^{2+}. We increased concentration of the metal to maximum until we observed differences in sorption activity among composites. Adsorption of Pb^{2+} was found to be efficient even for extremely high concentrations of this cation. The advantage of such sorbent is to keep maximum possible sorption activity for both groups of cations (heavy metals and radionuclides) and to have a good conductivity property to get multifunctional sorbent with a wider field of use.

2. Materials and methods

2.1. Chemicals

All purchased chemicals were of analytical grade. Kaolin, sodium silicate, lead nitrate and cadmium chloride hydrate were purchased from Sigma-Aldrich. NaOH was purchased from Penta. The natural graphite was obtained from Koh-i-Noor Grafit, Ltd, Czech Republic. The chemical reagents for synthesis of GO and GO-COOH, i.e. H$_3$PO$_4$, H$_2$SO$_4$, H$_2$O$_2$, KMnO$_4$ and chloroacetic acid were supplied from Lach-ner, Ltd. and Penta, Ltd. (Czech Republic). Radioactive source of cesium chloride (^{134}CsCl) and of strontium chloride (^{85}SrCl$_2$) were obtained from POLATOM, Poland. Demineralized (DEMI) water was used for all experiments.

2.2. Synthesis

Zeolites A, P and Y were prepared hydrothermally from kaolin (metakaolin) and NaOH by previously reported procedures.

Zeolite A: Preparation of the zeolite A was performed according to an already published procedure [26] but on a larger scale. 10.0 g metakaolin (kaolin annealed at 600 °C) was mixed with 120.0 mL NaOH (2.8 M), placed into an autoclave with a Teflon insert and heated at 100 °C for 4 h. Afterwards it was washed and centrifuged until constant pH was achieved. The product was dried overnight at 80 °C.

Zeolite P: 4.36 g of metakaolin (kaolin annealed at 600 °C) and 14. 39 Na$_2$SiO$_3$.5H$_2$O were placed into a Teflon liner. Into a Teflon beaker was prepared solution of 3.2 g NaOH and 80 mL DEMI water, stirred with a Teflon stirrer and transferred into a Teflon liner and placed into an autoclave. The reaction was conducted in an oven for 49 h at 106 °C. The obtained mixture was washed by DEMI water into constant pH and dried at 80 °C [26].

Zeolite Y: 1.6 g of metakaoline (kaoline annealed at 800 °C), 2.5 g NaOH, 16 mL DEMI water, were stirred together for 30 min. Into a Teflon beaker was added 4 g of Na$_2$SiO$_3$.5H$_2$O and 8 mL DEMI water and stirred for 30 min. The reactants were left stand for 24 h at room temperature (RT) and consequently placed into an autoclave with a Teflon liner and left to react at 100 °C for 9 h [27]. The autoclave was left to cool down in a turned off oven, the product was washed with water until constant pH, filtered and dried at 50 °C.

Graphene was prepared by exfoliation of 1 g natural graphite in 100 mL ethylene glycol in a high intensity cavitation field and pressure 5 bar for 20 min in a batch reactor UIP2000 (20 kHz, 2000W, HielscherUltrasonics, GmbH, Germany). The product was purified by dialysis (Spectra/Por3 dialysis membrane) in an ultrasonic bath in DEMI water [28].

Graphene prepared by ultrasound exfoliation was oxidized to graphene oxide by modified Hummers' method, which is safer but sufficiently effective. The small portions of graphene (in total 1 g) was added 60 mL H_2SO_4, 10 mL H_3PO_4 and oxidation reagent 3 g $KMnO_4$. Reaction mixture was stirred at 40 °C for 48 h. Afterwards, 1 g $KMnO_4$ was added and the mixture was stirred for additional 48 h and eventually poured on mixture of ice with 200 mL of 30 % H_2O_2. The resulting GO is purified by dialysis in ultrasound until constant pH~ 2.35 [29].

Carboxylated graphene was prepared by addition of 87 mL of GO suspension (0.0079 g/mL) and 100 mL DEMI water to 0.84 g of chloroacetic acid. Reaction mixture was heated to 110 °C stirred for 6 h [30]. Afterwards, it was stirred additional 120 h at RT. Reaction mixture was purified using Spectra/Por3 dialysis membrane to zero conductivity of water. Final GO-COOH suspension had pH 2.8 and concentration 0.0027 g/mL, it was therefore further concentrated by vacuum evaporation at 40 °C (final concentration 0.0079 g/mL).

The composites were prepared by a wet method. Synthesis of the composite Gr-GO-A started when water suspension of exfoliated graphite (11.8 mL, 0.017 g/mL) and graphene oxide (16.26 mL, 0.0123 g/mL) was sonicated in an ultrasonic bath for 5 min. The mixture was diluted by 40 mL DEMI water in order to get better homogenization, consecutively 0.1 g of zeolite was added and left under stirring for 24 h at RT. The resulting composite was isolated by vacuum evaporation. The other composites were prepared similarly. The ratio Gr-GO-zeolite (A, P or Y) was 40:40:20 weight percent except the sample Gr-GO-A-2 where the ratio was 25:25:50. In the case of composite Gr-GO-COOH-A, carboxylated GO was used instead of GO in the ratio 40:40:20.

2.3. Methods of characterization

All diffraction patterns were acquired using Bruker D2 (CuKα radiation, 30 kV, 10mA). The primary divergence slit module with 0.6 mm, Soller module 2.5, Ni Kbeta-filter 0.5 mm, step 0.00809° and time per step 1.0 were used in the range 5–90°.

FTIR spectra were measured on a Thermo Nicolet Nexus 670 FTIR spectrometer in the region of 4000–400 cm^{-1} at resolution of 4 cm^{-1}. Prior the measurement, the samples were pressed into a pellete with KBr.

Raman spectra were acquired using DXR Raman microscope (Thermo Scientific) with either a 532 nm green laser with power 0.2–3 mW for the most samples (slit 25 or 50 μm), under 10× objective of Olympus microscope.

Morphology of the samples was acquired by FEI Nova NanoSEM 450 high resolution scanning electron microscope equipped with a Through Lens detector (TLD) and an Everhart-Thornley secondary electrons detector (ETD). Prior the measurement, water suspension of the sample was deposited on a silicon chip substrate attached to an aluminum target and left to evaporate.

2.4. Sorption tests

Sorption of Sr^{2+} and Cs^+ was done by batch sorption method analogous to procedure reported by Bubenikova et al. [19]. The composites (0.01 g) were first pre-equilibrated with solutions in stoppered test tubes (contact time 24 h). The Sr^{2+} test solutions labelled with ^{85}Sr radiotracer (^{85}Sr activity 4 kBq/1.5 mL) or Cs^+ solutions labelled with ^{134}Cs radiotracer (^{134}Cs activity 6 kBq/1.5 mL) were added into suspension of composites and were shaken at temperature 25 ± 0.1 °C. The final volume (1.5 mL) and liquid-to-solid ratio (150 mL/g) was the same as in the case of previous published publication [19]. After filtration of the suspensions (mixed cellulose filters), aliquots of filtrate were measured. The automatic gamma counter Wallac 1480 WIZARD 3 (PerkinElmer Life Sciences, Wallac Oy) with NaI(Tl) well-type detector was employed. Every experiment was performed twice and the mean value was reported [19].

Sorption measurements of Pb^{2+} and Cd^{2+} were performed analogously as experiments with radionuclides except that no radiotracer

solution was added and metal concentrations were determined by atomic absorption spectroscopy.

The adsorption of metal, expressed as the uptake (%), was calculated by Eq. (1):

$$Uptake = \frac{A_0 - A}{A_0} \cdot 100 \tag{1}$$

where A_0 and A are relative activities of the solution of the isotope before and after contact with the adsorbent.

The adsorption isotherms were plotted as the dependence of the equilibrium concentration of the adsorbed ion on the adsorbent q_e (mmol/g), on their equilibrium concentration in the liquid phase c_e (mol/L). The equilibrium concentrations of the ions in liquid and solid phases were calculated by Eqs. (2) and (3):

$$C_e = \frac{A}{A_0} \cdot C_0 \tag{2}$$

$$q_e = \frac{A_0 - A}{A_0} \cdot \frac{V}{m} \cdot C_0 \tag{3}$$

where A_0 and A are relative activities of the solution before and after contact with the adsorbent, m is mass of adsorbent (g), V is volume of liquid phase (mL), c_0 is the initial concentration of the ion in the solution (mol/L).

The Freundlich and Langmuir adsorption isotherms were used for fitting of adsorption equilibrium data. Freundlich isotherm model can be calculated by Eq. (4):

$$q_e = K_F C_e^{1/n} \tag{4}$$

where K_F (mmol/g) and n are constants related to the adsorption capacity and adsorption intensity, respectively. The Langmuir isotherm model can be described by Eq. (5):

$$q_e = q_{max} \cdot \frac{K_L C_e}{1 + K_L C_e} \tag{5}$$

where q_{max} (mmol/g) is the maximum adsorption capacity and K_L (L/mmol) is a constant related to the affinity of the binding sites. The Freundlich and Langmuir isotherm constants were calculated by Origin software.

All kinetics experiments were performed from stock solutions with a concentration of 1×10^{-3} mol/L. For the determination of adsorption isotherms on Gr-GO-A-2 sample, solutions containing various concentrations of Cs^+ (1×10^{-5}–4×10^{-2} mol/L) and Sr^{2+} (1×10^{-5}–2×10^{-2} mol/L) in distilled water labelled by ^{134}Cs and ^{85}Sr isotope were prepared. Solutions prepared without radioactive labelling were used for experiments with heavy metals with concentrations of Cd^{2+} (1×10^{-5}–3.5×10^{-2} mol/L) and Pb^{2+} (1×10^{-5}–2.4×10^{-2} mol/L).

2.5. Voltammetric tests

To test composite's ability to provide suitable set of parameters required by paste electrode, differential pulse voltammetry experiment in solution containing Pb^{2+} and Cd^{2+} ions was done. The differential pulse voltammogram was measured with the zeolite/graphene paste electrode in water following the transfer of the electrode after the sorption period in stirred $PbCl_2$ and $CdCl_2$ solution (1.10×10^{-5} mol/cm³ and 1.71×10^{-5} mol/cm³ respectively, period length 3600 s).

3. Results and discussion

3.1. Structural characterization

The composites were prepared with defined ratio 40:40:20 for all composites Gr:GO:Z. The composite Gr-GO-COOH-A was prepared with

carboxylated GO instead of GO. One composite with zeolite A, denoted as Gr-GO-A-2, was exceptionally prepared in ratio 25:25:50 to see the limits of concentration of the active component GO.

The XRD patterns of the composites (Figure 1.) show presence of very intensive diffraction of Gr and medium intensive diffraction for GO. Presence of zeolites were confirmed by less intensive diffractions (see Fig. S1 for XRD patterns of individual components). Diffraction line (002) for GO shifts for some composites, which can indicate an effect on interplanar distance.

The FTIR spectra (Figure 2) contain bands for adsorbed water at 3424 and 1634 cm^{-1} corresponding to O–H stretching vibration of surface-adsorbed water, and vibration at $\sim$ 1008 cm^{-1} belongs to Si–O bond. From the missing band of C=O bond of carboxylic group at $\sim$ 1742 cm^{-1} can be concluded that vibration bands of GO are absent.

The Raman spectra of the composites (Figure 3) contain bands for GO at 1350 and 1594 cm^{-1} and in case of composites Gr-GO-A, Gr-GO-P and Gr-GO-Y also the most intensive band for Gr at 1576 cm^{-1}. No significant shift of vibrations was observed; intensity of D and G bands is in ratio $\sim$1:1.

3.2. Morphology

The SEM micrographs (Figures 4, 5, 6, 7, and 8) show that zeolites are surrounded by exfoliated graphite and the mixture is in all cases completely covered by well anchored GO sheets. It is evident that neither GO nor GO-COOH form aggregates. Different zeolite morphology is visible in Figures 4, 5, and 6. The overview images are shown to demonstrate better homogeneity of the composites (Figure 4a - Gr-GO-A, Figure 5a - Gr-GO-P, Figure 6a - Gr-GO-Y). The detail images are illustrating different morphology of each zeolite (Figure 4a - zeolite A, Figure 5a - zeolite P, Figure 6a - zeolite Y). The composites Gr-GO-COOH-A and Gr-GO-A-2 are seen in Figures 7 and 8. All SEM images show GO/GO-COOH well grafted on the zeolite and exfoliated graphite is possible to see also under the GO/GO-COOH sheets (overview images Figures 7a, 8a and detail images Figures 7b,8b).

3.3. Sorption experiments

The sorption results of Pb^{2+} and Cd^{2+} from solutions of initial concentration 0.001 mol/L are reported in Tables 1 and 2, respectively. All composites showed complete sorption of Pb^{2+}. Sorption of Cd^{2+} was also high but lower than for Pb^{2+}; the worst performance showed the composite Gr-GO-P that captured 91.9% of Cd^{2+}. Therefore, the type of zeolite affects sorption of Cd^{2+} in this case.

Sorption experiment was performed with significantly higher concentration of the initial solutions 0.022 mol/L (4.5 g/L of Pb^{2+}) $Pb(NO_3)_2$ in water and 0.027 mol/L (3 g/L of Cd^{2+}) $CdCl_2.H_2O$ in water in order to identify the best sorbent. The sorption results are reported in Tables 3

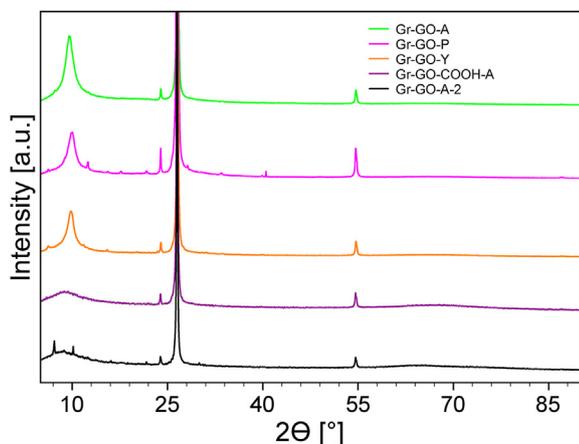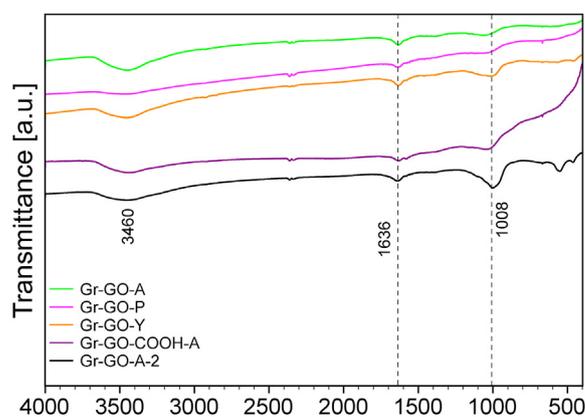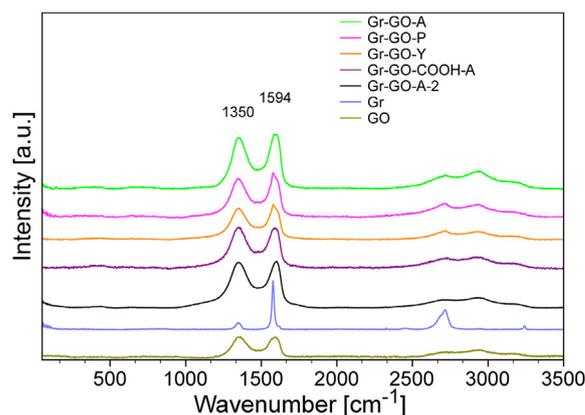**Figure 2.** FTIR spectra of all composites.

Figure 3. Raman spectra of all composites and pure graphene and GO.

and 4, respectively. The best sorbent for Pb^{2+} as well as Cd^{2+} with ratio of components Gr:GO:Z 40:40:20 contained zeolite A and carboxylated GO. This result was expected since GO-COOH contains more –COOH functional groups suitable for metal capture. From the composites with GO, the composite containing zeolite P showed the lowest sorption for both Pb^{2+} and Cd^{2+}. No significant difference in selectivity towards the investigated cations was observed for the composites. When the ratio of the components was changed to 25:25:50 for the composite with zeolite A and GO, sorption of Pb^{2+} and Cd^{2+} further increased.

Sorption of Cs^+ and Sr^{2+} from 0.001 mol/L solutions, shown in Tables 5 and 6, followed similar trends as heavy metals, i.e. the best sorbent Gr:GO:Z 40:40:20 containing zeolite A and carboxylated GO and the composite Gr:GO:A in ratio 25:25:50 performed even better, although the differences were small. No significant difference in selectivity towards the two cations was observed.

The FTIR spectra of all samples before/after Cd^{2+}/Pb^{2+} sorption are in Fig. S2-S6. The spectra of starting materials (GO and zeolites) for preparation of composites are also presented. The exfoliated graphite has no FTIR active vibration therefore the spectrum is not shown. Generally, the spectra of composites are not changing after sorption. The exception are spectra of Gr-GO-A after Cd^{2+} sorption, Gr-GO-Y after Cd^{2+} and Pb^{2+} sorption. The changes are in the region 900-1200 cm^{-1} which is corresponding to C–OH, C–O–C vibration bands of GO [30] and also to Si–O, Si–O–Al, Al–OH vibration bands of zeolites [31]. The SEM images of these three composites after sorption were collected (Fig. S7-S9) to better understand and to exclude decomposition of zeolites after sorption. All SEM images show that the zeolites are not decomposed. The explanation of changes in FTIR spectra could be easily explained by inhomogeneity of the sample. The composites contain some bearings with higher concentration
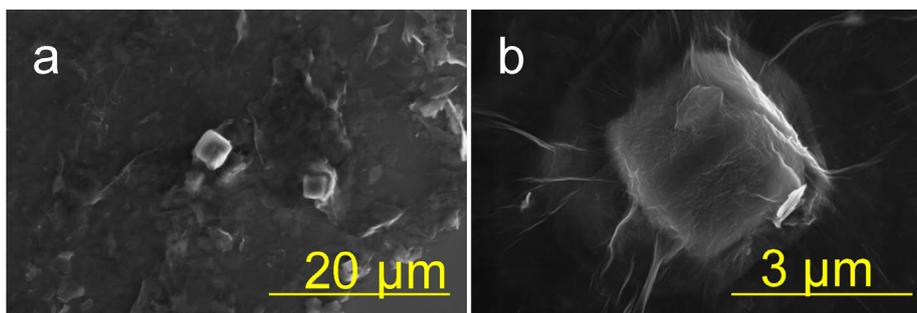

Figure 1. XRD patterns of all composites.

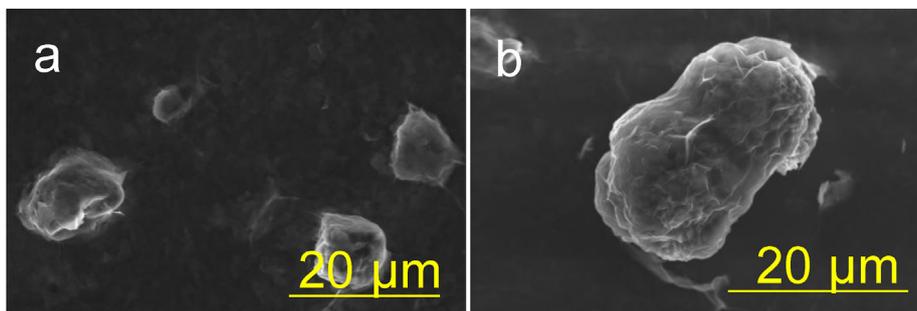**Figure 4.** SEM images of composite Gr-GO-A (a - overview, b - detail).

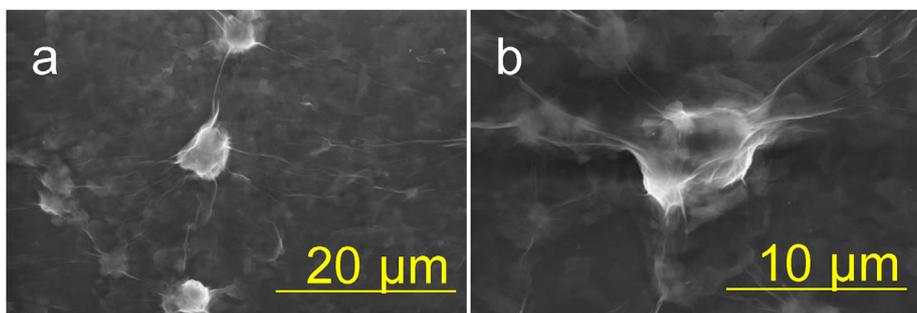**Figure 5.** SEM images of composite Gr-GO-P (a - overview, b - detail).

Figure 6. SEM images of composite Gr-GO-Y (a - overview, b - detail).
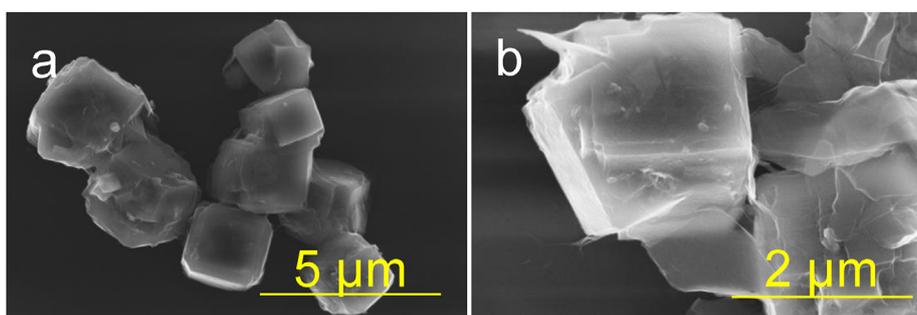

Figure 7. SEM images of composite Gr-GO-COOH-A (a - overview, b - detail).

of zeolites (Fig. S8-S9; Gr-GO-Y after Cd^{2+} and Pb^{2+} sorption) and with lower concentration of GO (Fig. S7; Gr-GO-A after Cd^{2+} sorption).

3.3.1. Kinetics studies

The effect of contact time on the adsorption for Gr-GO-A-2 sample is shown for Cd^{2+} and Pb^{2+} in Figure 9a, and for Cs^+ and Sr^{2+} in Figure 9b.

The percentage of uptake increased with increasing contact time and reached a constant value. The kinetics of Cs^+ adsorption was quite fast and the equilibrium was attained within 30 min. Similar results were observed for Sr^{2+} uptake. In contrast to these results, the kinetics of Cd^{2+} and Pb^{2+} uptake was slower and a longer time was required to reach equilibrium. In the case of Pb^{2+} adsorption, equilibrium was not reached even after 5 h.
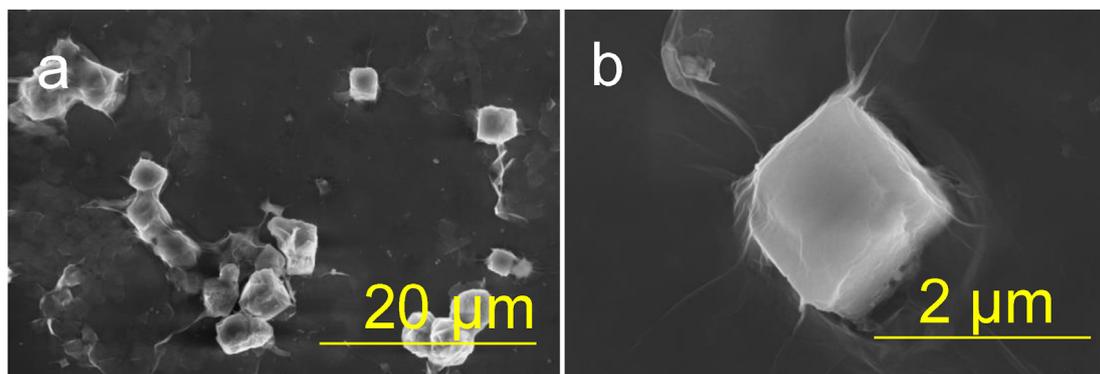
Figure 8. SEM images of composite Gr-GO-A-2 (a - overview, b - detail).

Table 1. Sorption of Pb^{2+} in water.

Sample	pH	Sorption [%]	K_d [ml/g]
Gr-GO-A	6.6	99.9 ± 0.1	>100000
Gr-GO-P	5.2	99.9 ± 0.1	>100000
Gr-GO-Y	6.1	100.0 ± 0	>300000
Gr-GO-COOH-A	7.0	100.0 ± 0	>300000
Gr-GO-A-2	7.7	100.0 ± 0	>300000

0.001 mol/L $Pb(NO_3)_2$ in water, V/m = 150 mL/g, contact time 24 h, T = 25 °C.

Table 5. Sorption of Cs^+ in water.

Sample	pH	Sorption [%]	K_d [ml/g]
Gr-GO-A	6.1	86.5 ± 0.3	966 ± 14
Gr-GO-P	5.4	90.4 ± 0.2	1412 ± 15
Gr-GO-Y	6.0	86.8 ± 0.2	992 ± 18
Gr-GO-COOH-A	6.7	96.1 ± 0.2	3691 ± 199
Gr-GO-A-2	7.2	96.2 ± 0.1	3790 ± 26

0.001 mol/L CsCl, V/m = 150 mL/g, contact time 24 h, T = 25 °C.

Table 2. Sorption of Cd^{2+} in water.

Sample	pH	Sorption [%]	K_d [ml/g]
Gr-GO-A	6.6	99.1 ± 0.1	16284.0 ± 112.3
Gr-GO-P	5.0	91.9 ± 0.1	1689.5 ± 11.0
Gr-GO-Y	6.1	99.1 ± 0.1	17169.2 ± 439.0
Gr-GO-COOH-A	7.0	100.0 ± 0	>400000
Gr-GO-A-2	7.7	100.0 ± 0	>1000000

0.001 mol/L $CdCl_2.H_2O$ in water, V/m = 150 mL/g, contact time 24 h, T = 25 °C.

Table 6. Sorption of Sr^{2+} in water.

Sample	pH	Sorption [%]	K_d [ml/g]
Gr-GO-A	5.9	98.2 ± 0.1	8415 ± 47
Gr-GO-P	5.1	89.9 ± 0.1	1345 ± 7
Gr-GO-Y	5.4	97.5 ± 0.1	5743 ± 151
Gr-GO-COOH-A	6.5	99.9 ± 0.1	146791 ± 39011
Gr-GO-A-2	6.8	99.9 ± 0.1	220162 ± 14969

0.001 mol/L $SrCl_2$, V/m = 150 mL/g, contact time 24 h, T = 25 °C.

Table 3. Sorption of Pb^{2+} in water.

Sample	pH	Sorption [%]	K_d [ml/g]
Gr-GO-A	4.3	11.7 ± 0.6	19.9 ± 1.2
Gr-GO-P	3.6	8.2 ± 0.8	13.4 ± 1.4
Gr-GO-Y	4.0	9.1 ± 3.0	15.2 ± 5.5
Gr-GO-COOH-A	4.2	21.7 ± 1.9	41.7 ± 4.4
Gr-GO-A-2	4.4	43.7 ± 0.5	117.0 ± 2.1

0.022 mol/L (4.5 g/L) $Pb(NO_3)_2$ in water, V/m = 150 mL/g, contact time 24 h, T = 25 °C.

Table 4. Sorption of Cd^{2+} in water.

Sample	pH	Sorption [%]	K_d [ml/g]
Gr-GO-A	5.6	7.9 ± 2.0	12.9 ± 3.6
Gr-GO-P	4.4	6.7 ± 2.9	10.9 ± 5.1
Gr-GO-Y	4.9	10.4 ± 1.1	17.5 ± 2.1
Gr-GO-COOH-A	5.5	12.1 ± 1.2	20.8 ± 2.5
Gr-GO-A-2	5.8	29.9 ± 0.1	63.9 ± 0.4

0.027 mol/L (3 g/L) $CdCl_2.H_2O$ in water, V/m = 150 mL/g, contact time 24 h, T = 25 °C.

3.3.2. Adsorption isotherms

The sorption capacity of studied samples increased with equilibrium concentrations raised of Pb^{2+} (Figure 10a), Cd^{2+} (Figure 10b), Cs^+ (Figure 11a) and Sr^{2+} (Figure 11b) in aqueous solutions, thus gradually saturating the adsorbent. The Freundlich and Langmuir isotherm models were used for analysis of experimental equilibrium data. The mechanism of adsorption could be associated with adsorption onto heterogenous surface (Freundlich isotherm model) or as monolayer adsorption onto surface with all the adsorption sites having the same sorption energy independent of surface coverage (Langmuir model) [19]. Table 7 shows the Freundlich and Langmuir gained by fitting the sorption equilibrium data.

Comparison of the coefficients of determination (R^2) shows that the sorption of Sr^{2+} and Cd^{2+} on Gr-GO-A-2 sample corresponds better to the Langmuir isotherm than to the Freundlich isotherm, indicating that the sorption of ions on the sorbent is monomolecular. Zeolite A prepared from coal fly ash was tested for sorption of Cs^+ and Sr^{2+} by Tian et al. In their case the Langmuir model described the experimental data better than the Freundlich model and the sorption capacity for Cs^+ was higher than for Sr^{2+} [32]. The maximum amount of ion adsorbed calculated from the Langmuir model corresponds to 1.306 mmol/g (173.6 mg/g) for Cs^+, 0.782 mmol/g (68.5 mg/g) for Sr^{2+}, 1.107 mmol/g (124.4 mg/g) for Cd^{2+} and 1.205 mmol/g (249.7 mg/g) for Pb^{2+}. In contrast, in the case of Cs^+ and Pb^{2+} adsorption, the R^2 values are higher for the Freundlich model and therefore the fit to the measured experimental data is more
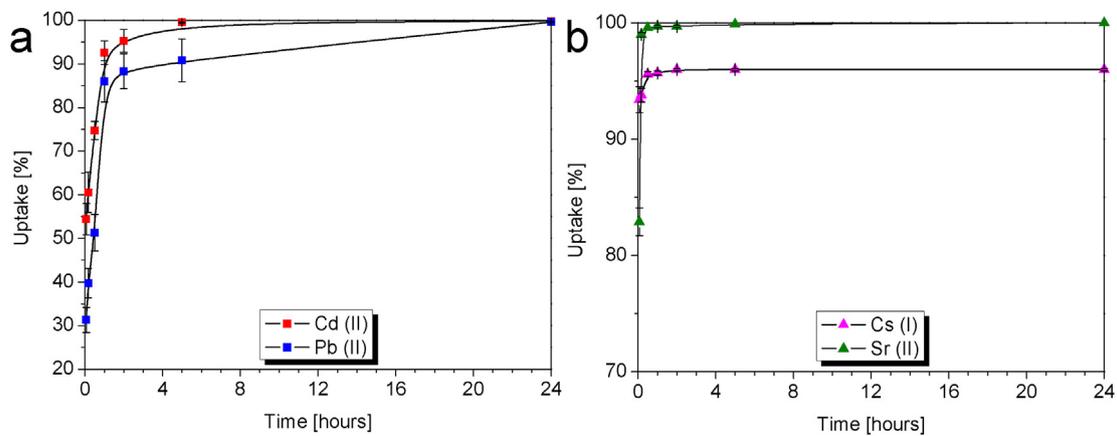
Figure 9. Pb^{2+}, Cd^{2+} (a) and Cs^+, Sr^{2+} (b) adsorption kinetics for Gr-GO-A-2 sample.
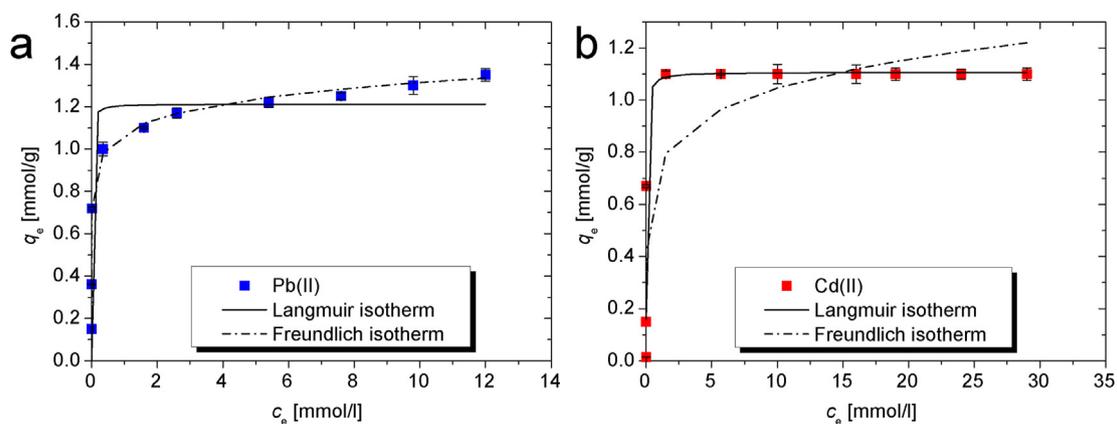

Figure 10. Pb^{2+} (a) and Cd^{2+} (b) adsorption isotherms for Gr-GO-A-2 sample.
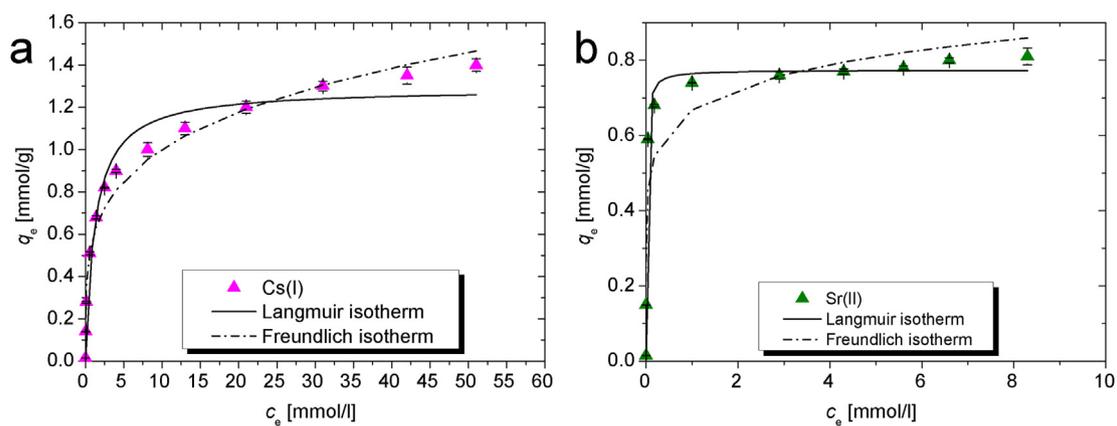

Figure 11. Cs^+ (a) and Sr^{2+} (b) adsorption isotherms for Gr-GO-A-2 sample.

Table 7. A comparison of Freundlich and Langmuir isotherm constants for the sorption of Cs^+, Sr^{2+}, Cd^{2+} and Pb^{2+} from aqueous solutions on Gr-GO-A-2.

Metal	Freundlich model			Langmuir model		
	K_F (mmol/g)	n	R^2	q_{max} (mmol/g)	K_L (mmol/L)	R^2
Cs^+	0.585	4.282	0.974	1.306	0.764	0.960
Sr^{2+}	0.653	7.701	0,905	0.782	86.580	0.988
Cd^{2+}	0.751	6.926	0.775	1.107	38.154	0.926
Pb^{2+}	1.075	11.508	0.901	1.205	155.16	0.853

accurate. Jangkorn et al. investigated adsorption of Pb^{2+} on zeolite prepared from bagasse fly ash and coal fly ash. The adsorption isotherms in this case were better explained by Langmuir model than by Freundlich model [33].

3.4. Voltammetric experiment

Parameters of the differential pulse voltammetry measurement (Fig. S10) were as following: initial reduction phase 10 s at -1,4 V vs. OCP

(Open Circuit Potential), potential range of anodic sweep -1.4 V–0 V vs. OCP, step 0.005 V, modulation time 0.05 s, modulation amplitude 0.025 V. Peaks at -0,4 V and -0,2 V vs. OCP respectively can be attributed to the oxidation reactions of pre-reduced Cd and Pb. Thus, the results demonstrate usability of the composite as the filling of the paste electrode and further study of this potential usage is underway.

4. Conclusions

In this paper, composites of graphene/graphene oxide with three zeolites were synthesized, characterized and their sorption efficiency was compared. Structure of the composites was determined from XRD, FTIR and Raman measurements. Diffraction patterns and spectra of individual components were measured as well and compared to literature. XRD results confirmed presence of all three components. The zeolites show just the most intensive diffractions while diffractions of graphene and graphene oxide were dominant. The Raman spectroscopy was useful to provide information about quality of graphene/GO sheets in the composites. The SEM micrographs confirmed that zeolites of all types were surrounded by exfoliated graphite with GO anchored to surface.

In general, the composites showed high sorption activity of all investigated cations from 0.001 mol/L solutions. The differences of sorption among the composites were only seen by testing higher concentration solutions. Extreme high concentrations of Pb^{2+} and Cd^{2+} (0.022 mol/L and 0.027 mol/L) were needed to observe difference in sorption properties among the composites. The best sorbent for all cations with ratio 40:40:20 belongs to the Gr-GO-COOH-A. When the ratio of the components was changed to 25:25:50 for the composite Gr:GO:A, sorption further increased. Therefore, due to good sorption properties of these two composites towards selected heavy metals as well as radionuclides, Gr-GO-COOH-A and Gr-GO-A-2 are suitable multifunctional sorbents.

The FTIR spectra of composites after Cd^{2+}/Pb^{2+} sorption was measured to see any interaction with cations or to see any structural changing. The C=O vibration is not clearly seen in composite spectra therefore it was impossible to say anything about the cation interaction with carboxylic group. Anyway, the region ~900-1200 cm^{-1} corresponding to vibration bands of GO (C–OH, C–O–C) and zeolites (Si–O, Si–O–Al, Al–OH) seems to belong to inhomogeneity of the sample. Respectively, the SEM images after sorption prove that some selected part of composite contain bearings with higher concentration of zeolite composites (Gr-GO-Y after Cd^{2+} and Pb^{2+} sorption) or other composite GO which is not everywhere well grafted (Gr-GO-A after Cd^{2+} sorption).

The kinetics of Cs^+ and Sr^{2+} removal on Gr-GO-A-2 sample was fast and the equilibrium was reached approx. in 30 min. The kinetic of Cd^{2+} and Pb^{2+} removal was slower, the equilibrium for Pb^{2+} adsorption was not reached even after 5 h.

The adsorption isotherms were measured for Gr-GO-A-2 sample. The sorption results of Sr^{2+} and Cd^{2+} correspond better to the Langmuir isotherm than to the Freundlich isotherm. It could be concluded that the process corresponds to monolayer adsorption. The case of Cs^+ and Pb^{2+} adsorption data correspond to adsorption onto heterogenous surface (Freundlich model).

The results of measurements of the differential pulse voltammetry for Cd^{2+} and Pb^{2+} show that zeolite/graphene based composites have high potential to be used as paste electrode.

Generally, it could be concluded that the zeolite/graphene based composites are suitable to be used as a good sorbent for heavy metals and radionuclides and also for paste electrode.

Declarations

Author contribution statement

Darina Smržová: Performed the experiments; Analyzed and interpreted the data; Wrote the paper.

Lórant Szatmáry, Petra Ecorchard: Conceived and designed the experiments; Analyzed and interpreted the data; Wrote the paper.

Aneta Machálková; Petra Salačová: Performed the experiments.

Monika Maříková: Contributed reagents, materials, analysis tools or data.

Martin Straka: Conceived and designed the experiments; Performed the experiments; Analyzed and interpreted the data.

Data availability statement

The data that has been used is confidential.

Declaration of interest's statement

The authors declare no competing interests.

Additional information

Supplementary content related to this article has been published online at https://doi.org/10.1016/j.heliyon.2022.e12293.

References

[1] A.L. Ciosek, G.K. Luk, Kinetic modelling of the removal of multiple heavy metallic ions from mine waste by natural zeolite sorption, Water 9 (2017) 482.

[2] R.O. Abdel Rahman, A.M. El-Kamash, Y.-T. Hung, Applications of nano-zeolite in wastewater treatment: an overview, Water 137 (14) (2022) 1–30.

[3] M. Kragovic, A. Dakovic, M. Markovic, J. Krtic, G.D. Gatta, N. Rotiroti, Characteization of led sorption by the natural and Fe(III)-modified zeolite, Appl. Surf. Sci. 283 (2013) 764–774.

[4] Z. Ezzedine, I. Battoneau-Gener, Y. Pouilloux, H. Hamad, Z. Saad, Synthetic NaX zeolite as a very efficient heavy metals sorbent in batch and dynamic conditions, Coll. Interf. 2 (2018) 22.

[5] M.M. Llanes-Morter, M.T. Olguin, M.J. Solache-Rios, Lead sorption by a Mexican clinoptilolite-rich tuff, Environ. Sci. Pollut. Res. 14 (2007) 397–403.

[6] F. Arrelano, I. Garcia-Sosa, M. Solache-Rios, Sorption of Co and Cd by zeolite Y, J. Radioanal. Nucl. Chem. Lett. 199 (1995) 107–113.

[7] D. Alby, C. Charnay, M. Heran, B. Prelot, J. Zajac, Recent developments in nanostructured inorganic materials for sorption of cesium and strontium: synthesis and shaping, sorption capacity, mechanisms, and selectivity- review, J. Hazard Mater. 344 (2018) 511–530.

[8] B.S. Barus, K. Chen, M. Cai, R. Li, H. Chen, C. Li, J. Wang, S.-Y. Cheng, Heavy metal adsorption and release on polystyrene particles at various salinities, Front. Mar. Sci. 8 (2021), 671802, 1-14.

[9] M. Xu, Y. Cai, G. Chen, B. Li, Z. Chen, B. Hu, X. Wang, Efficient selective removal of radionuclides by sorption and catalytic reduction using nanomaterials, Nanomaterials 12 (2022) 1443, 1-18.

[10] A.S. Diamantis, A.D. Pournara, E.D. Koutsouroubi, C. Moularas, Y. Deligiannakis, G.S. Armatas, A.G. Hatzidimitriou, M.J. Manos, T. Lazarides, Detection and sorption of heavy metal ions in aqueous media by a fluorescent Zr(IV) Metal−Organic framework functionalized with 2-picolylamine receptor groups, Inorg. Chem. 61 (2022) 7847–7858.

[11] N. Boulanger, A.S. Kuzenkova, A. Iakunkov, A.Y. Romanchuk, A.L. Trigub, A.V. Egorov, S. Bauters, L. Amidani, M. Retegan, K.O. Kvashnina, S.N. Kalmykov, A.V. Talyzin, Enhanced sorption of radionuclides by defect-rich graphene oxide, ACS Appl. Mater. Interfaces 12 (2020) 45122–45135.

[12] M. Arancibia-Miranda, S.E. Baltazar, A. Garcia, D. Munoz-Lira, P. Sepulveda, M.A. Rubio, D. Altbir, Nanoscale zero valent supported by Zeolite and Montmorillomite: template effect of the removal of lead ion from an aqueous solution, J. Hazard Mater. 301 (2016) 371–380.

[13] P.K. Pandey, S.K. Shara, S.S. Sambi, Removal of lead (II) from waste water on zeolite NaX, J. Environ. Chem. Eng. 3 (2015) 2604–2610.

[14] S. Salem, A. Salem, A novel design for clean and economical manufacturing new nano-porous zeolite based adsorbent by alkali cement kiln dust for lead uptake from wastewater, J. Clean. Prod. 143 (2017) 440–451.

[15] H.-M. Yang, C.W. Park, I. Kim, I.-H. Yoon, Y. Sihn, Sulfur-modified chabazite s a ow-cost ion exchanger for the highly selective and simultaneous removal of cesium and strontium, Appl. Surf. Sci. 536 (2021), 147776.

[16] H. Faghihian, M. Moayed, A. Firooz, M. Iravani, Synthesis of a novel magnetic zeolite nanocomposite for removal of Cs^+ and Sr^{2+} from aqueous solution: kinetic, equilibrium and thermodynamic studies, J. Colloid Interface Sci. 393 (2013) 445–451.

[17] J. Liu, Z.J. Huang, J. Sun, Y.X. Zou, B.N. Gong, Enhancing the removal performance of Cd(II) from aqueous solutions by NaA zeolite through doped thiourea reduced GO which is trapped within zeolite crystals, J. Alloys Compd. 815 (2020), 152514.

[18] Y. Shi, X. Ren, H. Zheng, Y. Zhang, Q. Zuo, Hierarchical 13X zeolite/reduced graphene oxide porous materials for trace Pb(II) capturing from drinking water, Microporous Mesoporous Mater. 329 (2022), 111540.

[19] M. Bubenikova, P. Ecorchard, L. Szatmary, O. Mrozek, P. Salacova, J. Tolasz, Sorption of Sr(II) onto nanocomposites of graphene oxide-polymeric matrix, J. Radioanal. Nucl. Chem. 315 (2018) 263–272.

[20] D. Zheng, H. Hu, X. Liu, S. Hu, Application of graphene in electrochemical sensing, Curr. Opin. Colloid. In. 20 (5-6) (2015) 383–405.

[21] I. Svancara, K. Kalcher, A. Walcarius, K. Vytras, Electroanalysis with Carbon Paste Electrodes, 2012.

[22] I. Švančara, K. Vytřas, J. Barek, J. Zima, Carbon paste electrodes in modern electroanalysis, Crit. Rev. Anal. Chem. 31 (4) (2001) 311–345.

[23] J. Lehto, R. Koivula, H. Leinonen, E. Tusa, R. Harjula, Removal of radionuclides from fukushima daiichi waste effluents, Separ. Purif. Rev. (2019) 1–21, 00.

[24] J.U. Ahmad, M.A. Goni, Heavy metal contamination in water, soil, and vegetables of the industrial areas in Dhaka, Bangladesh, Environ. Monit. Assess. 166 (2010) 347–357.

[25] R. Gusain, N. Kumar, E. Fosso-Kankeu, S.S. Ray, Efficient removal of Pb(II) and Cd (II) from industrial mine water by a hierarchical MoS2-SH-MWCNT nanocomposite, ACS Omega 4 (2019) 13922–13935.

[26] R.D. Bessa, L.D. Costa, C.P. Oliveira, F. Bohn, R.F. Do Nascimento, J.M. Sasaki, A. Rodrigues-Loiola, Kaolin-based magnetic zeolite A and P as water softeners, Microporous Mesoporous Mater. 245 (2017) 64–72.

[27] L.B. Bortollato, R.A.A. Boca Santa, J.C. Morcira, D.B. Machado, M.A.P.M. Martins, M.A. Fiori, N.C. Kuhnen, H.G. Riella, Synthesis and characterization of Y zeolites from alternative silicon and aluminum sources, Microporous Mesoporous Mater. 248 (2017) 214–221.

[28] V. V. Stengl, Preparation of graphene by using an intense cavitation field in a pressurized ultrasonic reactor, Chem. Eur J. 18 (2012) 14047–14054.

[29] V. Stengl, J. Henych, M. Vomacka, Slusna, doping of TiO2-GO and TiO2-rGO with noble metals: synthesis, characterization and photocatalytic performance for azo dye dicoloration, Photochem. Photobiol. 89 (2013) 1038–1046.

[30] J. Ederer, P. Janos, P. Ecorchard, V. Stengl, Z. Belcicka, M. Stastny, O. Pop-Georgievski, V. Dohnal, Quantitative determination of acidic groups in functionalized graphene by direct titration, React. Funct. Polym. 103 (2016) 44–53.

[31] W. Rondón, D. Freire, Z. Benzo, A.B. Sifontes, Y. Gonzáles, M. Valero, J.L. Brito, Application of 3A zeolite prepared from Venezuelan kaolin for removal of Pb (II) from wastewater and its determination by flame atomic absorption spectrometry, Am. J. Anal. Chem. 4 (2013) 584–593.

[32] Q. Tian, K. Sasaki, Application of fly ash-based materials for stabilization/ solidificatio by cesium and strontium, Environ. Sci. Pollut. Control Ser. 26 (2019) 23542–23554.

[33] S. Jangkorn, S. Youngme, P. praipitat, Comparative lead adsorptions in synthetic wastewater by synthesized zeolite A of recycled industrial wastes from sugar factory and power plant, Heliyon 8 (2022), e09323.